## Authors response on review of revised version of "Simultaneous observations of NLC and MSE at midlatitudes: Implications for formation and advection of ice particles" by Michael Gerding et al. Anonymous Referee #2

*We thank the reviewer for taking the time and for providing detailed comments. Answers to the specific comments are given one-by-one below (in italics). New line numbers refer to the manuscript with marked changes.*

The manuscript has improved during revision, especially regarding the recognition of PMSE physics and explanation of the examples shown. Corrections or extensions were applied to the manuscript where necessary. Although the authors answered to all questions, I have subsequent questions or comments to their extensions, as explicated below. The study of NLC and MSE lower and upper edges certainly is of scientific significance (even if no substantial new concepts, ideas, methods or datasets are introduced in the manuscript), especially in comparison to the respective results at polar latitudes, as this might give indications for different formation processes.

*We are happy that the reviewer acknowledges the scientific significance of this study. We would like to note that the presented data set of 7 years of simultaneous NLC and MSE records at midlatitudes is unique and has not been described before. The method is by intention similar to the method of Kaifler et al., 2011, and takes limitations for our smaller data set into account.*

Yet this remains a difficult task and the authors tried their best to supply with temperature and wind data, but the results are inconclusive. The question is still open whether the dataset is large enough to derive significant results and allow for interpretation. At some places, analysis that could aid interpretation is lacking, or results are not properly acknowledged.

*We agree that the data set is still comparatively small and interpretation needs some care. Therefore, we limit our conclusions. For example, Kaifler et al. subdivided their (much larger) data set into various subcategories, where we only had one category. We still think that our data set supports our conclusions. We prove this statement in detail below.*

I also want to make aware that the manuscript does not conform to the journals data policy, requesting the used datasets to be publically available in an online repository and to be cited accordingly.

*We decided to make the data publically available on an ftp server. Reference is added in the Acknowledgments.*

Layer thickness: There are several references to layer thickness throughout the text, however it was not analyzed. It is expected to be thin, but e.g. Fig 2d shows a rather thick layer. As it is just a combination of two analyzed variables, z_up - z_low, the effort to calculate at least mean values for NLC and MSE should not be unreasonable. It would aid interpretation to know if the layers are thinner than at polar latitudes. The authors suspect that, but can easily derive it from data.

*So far, we feared that such a plot might add too few information. We are happy to present it now (new Figure 6). Mean layer thicknesses are 1.35 km (NLC) and 1.89 km (MSE), in agreement with the mean upper and lower edges. Especially the MSE layer*

*is much thinner than at high latitudes (mean ~5 km, Kaifler et al., 2011). Some profiles show a thickness of more than 4 km, but as already mentioned in the description of Fig. 2d, these are rare occasions. The description of the new Fig. 6 starts on page 9, line 12.*

I think another flaw of the previous type was introduced during revision. In p. 12, l. 16: Kaifler et al. (2011) list z_low as 82.1 km which is not 0.5 km above the mid-latitude value of 82.6 km, but below. Thus it can not be explained by the general increase of NLC altitude with latitude. With about 50 m per degree of latitude the z_low from high latitude of 82.1 km would shift down to 81.4 km, and not up to 82.6 km. Furthermore, this cited increase with latitude refers to the centroid altitude, and it is not clear at all what applies for lower edges. Again, some more intelligence on this topic might be revealed by the analysis of the layer thickness.

*We apologize for the confusion of high- and mid-latitude numbers and the, therefore, erroneous explanation. Indeed, the lower edge at high latitudes is 500 m below (!) the lower edge at mid-latitudes. To some extent, the good agreement between lower edges of NLC and MSE at both locations is related to the thresholds used for selection of the data. For ALOMAR, Kaifler et al. (2011) have set the MSE threshold to 5 dB relative signal power and the NLC threshold to ß>4 $*10^{-10}$ /m/sr. For Kühlungsborn, we chose a MSE threshold of -12 dB SNR and a NLC threshold of ß>0.3$*10^{-10}$ /m/sr, based on the noise limit of the data. From Fig. 5 of Kaifler et al., the altitude change of lower and upper edges depending on the threshold for data selection can be seen. For NLC, we find similar dependencies also for our site, i.e. increasing the brightness limit for our data set lowers the mean NLC lower edge by a few 100 m. This is because bright NLC are typically found at lower altitudes, as also the reviewer stated below.*

*We would like to point out that the data selection results in a systematic difference of lower edge altitudes of a few 100 m. The upper NLC edges are affected similarly, but the difference is smaller (found by Kaifler et al. as well as in our data set). The upper edge of only the strong MSE is indeed expected to be lower than the upper edge of all MSE. But this altitude change is still much smaller than the difference found between high and mid latitudes.*

*Please note that the event selection described above is based on the signal maxima. After the selection process in Kaifler et al. (2011), the particular edges are identified at a lower signal level. For Kühlungsborn the data selection threshold and the edge threshold are set the same. We have demonstrated in Fig. 9 (new number) that the mean edge height of MSE depends only weakly on the edge threshold.*

*We have changed the erroneous description of the lower edge comparison and provide a discussion of the edge altitudes and their threshold dependence (p. 13, l. 3-6).*

Related to this topic is another missing quantity which is z_up for the complete MSE dataset. It is very important for interpretation and should not be omitted. The authors hint that it could be significantly larger than 84.5 km which is z_up of NLC during MSE. This would mean that high-altitude MSE are suppressed during NLC conditions, which would be a major result. I don't think the authors interpretation is correct, they state that the small particles at high altitudes have grown and sedimented and are thus removed from high altitude during NLC conditions. But this process would not suppress subsequent reformation of local (!) high-altitude MSE, as is obviously observed during non-NLC conditions.

*In the figure below we compare the occurrence of MSE at a particular altitude bin for our data set (simultaneous with NLC) and for all MSE (as published by Zecha et al., 2003). Normalization is different, but it can be easily seen that the fraction of high-reaching MSE is larger in the data set without separation. (Dashed lines are drawn to guide the eye.) We hesitate to provide a number for z_up for the complete data set because it includes many hours of MSE without lidar observations, i.e. likely mixing conditions with and without NLC. The evaluation of the complete MSE data set is in fact out of the scope of this paper. The low MSE layer width indeed says that high-altitude ice clouds rarely exist together with the comparatively low NLC (cf. new Figure 6). The relevance of sedimentation is well established and, e.g., presented by Rapp and Thomas (2006) and Kiliani et al. (2013). At higher latitudes the reformation of local high altitude (P)MSE may occur, because the height range of supersaturation is typically much larger. At mid-latitudes we expect a thinner supersaturated region (e.g. Gerding et al., 2007), and therefore low-altitude NLC/MSE and high-altitude MSE rarely exist at the same time at a particular location. We tried to sketch this in Figure 8 (new number).*

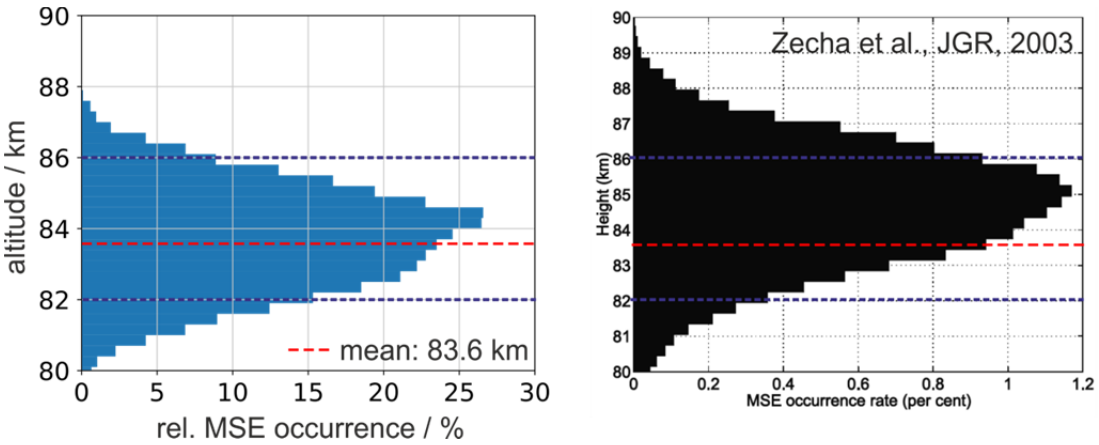


The fact that most NLC had to be discarded due to missing MSE is another major result, which I think is different from polar latitudes. I understand that the authors refrain from analyzing occurrence frequencies for good reason (limited statistics), but the total hours of NLC during daylight (ionization) discarded due to missing MSE could be robust, and it would be an important result.

*Indeed, it would be very interesting to learn about missing MSE if the ice is confirmed. Unfortunately it is only a very limited data set. If cases with too low solar elevation are excluded, the large majority of NLC are accompanied by MSE.*

*From the total number of NLC profiles, about 35% are observed during solar elevation below 5°(i.e. presumably too low ionization), about 20% are too weak (ß< $0.3*10^{-10}$ /m/sr, see Fig. 4 in Gerding et al., JGR, 2013). From the remaining part some fraction is discarded because radar is switched off. Then some few profiles remain, where either turbulence is missing, the ionization it still too low (unlikely), or the radar signal was below the threshold (lidar and radar signals depend different on particle size and number density). Given the complexity of MSE signal creation, we think only very limited conclusions can be drawn from the data set that is much smaller than the data set presented here.*

*We provide a more detailed description of the reasons to discard a large part of the NLC data (p. 7, l. 18-21).*

Representativeness for all NLC: I still wonder about the numbers, and the reason for the discrepancy between the NLC statistics of centroid height of 82.6 km and the MSE-selected NLC centroid height of 83.3 km. Looking at the distribution in Fig. 4a this seems to be a significant discrepancy not related to geophysical variance. The authors mention the removal of NLC during nighttime. This cannot be the reason, as Gerding et al. (2013) show rather slightly higher NLC centroid altitude during night, so this should not be an effect of diurnal variation. They mention the removal of weak NLC profiles during the beginning and end of the measurement, but this assumes they are at low altitude, which was not shown and which I doubt, as at polar latitudes NLC are brightest at low altitude. Then they mention the removal of very low NLC due to absence of MSE. Now this speaks for a strong coupling of NLC and MSE in line with the observations of coincident edges, and for a true (regarding physics) difference between NLC with and without MSE. Then the selection is not representative, but it does not have to be, this altitude-dependence of NLC regarding MSE conditions would rather be a major result of this study, if robust. Because Kaifler et al. (2011) found no such difference in NLC altitude due to PMSE selection, their table lists 82.1 km for both.

> *The difference between the mean peak height of the MSE-selected NLC (83.3 km, Fig. 4) and all 2010-2016 NLC (82.8 km, see p. 12, l. 17) is 0.5 km, i.e. half of the bin width used in the histograms. Both values are within the "most-probable" bin. We do not estimate this "significant", but see the NLC selected here as representative for all, within the geophysical variability and the context of this study. The diurnal variation of NLC altitudes described by Gerding et al. (2013) has indeed a minimum during the day. But the occurrence rate needs to be taken into account, which has a maximum in the early morning and a minimum in the evening. Indeed, bright NLC are typically lower than weak NLC. But this does not hold completely true when the NLC vanishes at low altitudes as can be seen in Fig. 2 a and b. The "removal of very low NLC due to absence of MSE" happens in a few cases. Unfortunately our data set is too small to conduct a systematic study.*

When the authors claim that 600 or 700 m is within the accuracy or variability or due to the limited size of the dataset, then this also applies to the upper edges, and it would be even more difficult to draw conclusions from these numbers given the large uncertainty. Then I would conclude that the dataset is yet too small to derive results that can aid understanding of the formation processes.

> *We see a geophysical variability of a few hundred meters, depending on selection of the data. We did an analysis of mean layer peaks, upper and lower edges for different sub-datasets with ~1000 NLC and MSE profiles (random sub-samples as well as sub-blocks). We found a distance of upper edges of NLC and MSE between 200 m and 700 m. Therefore we judge the difference to the situation at high latitudes significant, where the mean distance of upper edges is 3.3 km. We add a statement about the variability within subsets in the Discussion (p. 13, l. 11-15).*

The authors main conclusion is that mature NLC particles are advected to the observation site. While this may be true, and was claimed before, it is not totally clear if this conclusion is confirmed by the absence of MSE above the NLC layer (coincidence of upper edges) and if it can thus be strengthened by this study. For all we know, the particles could nucleate and grow within the NLC layer, or they could nucleate above the NLC layer but MSE could be suppressed by other mechanisms. So I am not yet convinced that the presented analysis allows for conclusive interpretation on this topic.

*Extensive nucleation within the NLC layer is unlikely because the supersaturation is typically too small. Typically, nucleation starts close to the mesopause, where supersaturation is largest. Ice clouds not visible as MSE may exist, but this would mean a systematic lack of turbulence in this height region (but not in the height of the NLC). We cannot exclude this due to lacking observations, but estimate it to be unlikely.*

I am looking forward to the authors thoughts and data on the points I mentioned. In case a second revision should be prepared, I give the following advice for improvements of the text. Especially in the conclusion a number of formulations are imprecise or incorrect:

p. 13, l. 20 and p. 15, l. 5: This should be expressed more carefully. There are no temperature measurements available at the lower edge at mid-latitudes. So the fact that the lower edges coincide hints at a large temperature gradient. This is not the same than expecting coincident edges on the assumption of a large temperature gradient.

*The reviewer is right that we do not have temperature measurements right below the NLC/MSE available for the events described here. But we have examined the temperature above and below the NLC earlier (Gerding et al., JGR, 2007) and found a saturation ratio of typically 0.1 about 1 km below the ice cloud. Even under climatological conditions with generally less pronounced gradients (Gerding et al., ACP, 2008) the temperature gradient at 80 km in summer results in a ~30% decrease of saturation within 200 m, assuming a constant water vapor pressure. We add "typically rising temperatures" to make clear that this assumption is well justified (p. 14, l. 12).*

p. 15, l. 8: "the layer is thinner": thickness was not evaluated, and no numbers were given for MSE-only. So we don't really know if it is thinner.

*We added a figure as suggested above. Additionally we changed "layer" to "ice cloud" to be more precise (p. 15, l. 18).*

p. 15, l. 10: "thin layer above" does this mean between the NLC top and the MSE top? But the smaller particles reach down to the NLC bottom. "no such layer at all" does that mean NLC without MSE, or coinciding upper edges?

*We rephrased to „Clouds that already exist long enough to form large particles (NLC) show only a thin layer of small particles (invisible for the lidar but visible as MSE) above the NLC at our site. Or they show no particles at all above the NLC, i.e. the upper edges of NLC and MSE coincide." (p. 15, l. 19 – p. 16, l. 3)*

p. 15, l. 12: "southward or northward or weak". There is no preference from the analysis, I'd say.

*We agree and changed the phrasing to "Meridional winds above the NLC do not show a preferential direction for the examined events." (p. 16, l. 4/5)*

p. 15, l. 13: if they don't grow to optically visible sizes, local formation of NLC is not possible

*We deleted "NLC".*

The language could be improved regarding expressions as "provides some rough information", "scattering happens only on structures" , "layers stretch much higher than", "revealed from PMSE observations", "particles have been grown to sizes", "we partly find very large agreement"

*We have rephrased these expressions*

p. 1, l. 19: For sure, PMSE have not been observed for several decades by human eye. I see that this happened during revision, but nevertheless strongly advise to pay attention to correctness of sentences.

We have changed the phrasing (p. 1, l. 20-23).

p. 2, l. 14: Thomas (2003) formulated a question, and Russell et al. (2014) make no reference to climate change at all. This topic might be too complex to be covered in half a sentence, so I suggest to remove this statement.

*We have removed the statement about climate change (p. 2, l. 15/16).*

p. 6, l. 3: the lower edges do not agree, they are plus or minus 1 km.

*We have removed the statement about the lower edges (p. 6, l. 3).*

p. 8, l. 9: indeed I can imagine this (Fig. 2d, 3:30 UT) to be a FOV effect

*We agree. Unfortunately a final answer on this can not be given.*

p. 8, l. 11: one could estimate the drift time given typical wind and FOVs, should be few minutes only.

*We added an example for the drift time under the assumption of 20 m/s wind speed (~3.5 min, p. 8, l. 14/15).*

p. 11, l. 20: my interpretation would be that there is no preference for any wind direction above the NLC layer.

*We agree that there is no significant preference, and changed the phrasing in the summary accordingly (p. 16, l. 5).*

Technical:

p. 1, l. 1: suggesting: “We combined ground-based lidar observations of noctilucent clouds (NLC) with colocated, simultaneous radar observations of mesospheric summer echoes (MSE) at a mid-latitude site in order to compare ice layer altitudes. While larger ice particles (> 10 nm) are directly observed by lidar, the echoes recorded by radar are created by a complex interplay of ice particles, ionization and turbulence. The combined lidar and radar dataset thus includes some information on the size distribution and history of the clouds. ..”

*We rephrased the first sentences to “We combined ground-based lidar observations of Noctilucent Clouds (NLC) with collocated, simultaneous radar observations of Mesospheric Summer Echoes (MSE) in order to compare ice cloud altitudes at a mid-latitude site (Kühlungsborn/Germany, 54° N, 12° E). Lidar observations are limited to larger particles (>10 nm), while radars are also sensitive to small particles (<10 nm), but require sufficient ionization and turbulence at the ice cloud altitudes. The combined lidar and radar data set thus includes some information on the size distribution within the cloud and by this on the 'history' of the cloud.”*

p. 1, l. 3: “first comparative study”: “first” could be removed, as it is not clear if the authors claim to do this for the first time, or if they plan a second study

*Changed, see above.*

p. 1, l. 6: “rough information”-> “Thus, some information on the size distribution and history of the cloud is included in the combined lidar and radar dataset.” Just a suggestion

*Changed, see above.*

p. 1, l. 10: “We find no difference of the lower edges”, as the accuracy of the radar is 300 m.

*New phrasing: “On average, there is no difference between the lower edges …”.*

p. 1, l. 13: “stretch higher” -> reach higher?

*Changed.*

p. 1, l. 17: I would turn this around: “High-altitude MSE, usually indicating nucleation of ice particles, are rarely observed in conjunction with lidar observations of NLC at Kühlungsborn.”

*We changed the phrasing. Thank you.*

p. 2, l. 6: “Later on” this might refer to the 1996 citation, but the 2017 citation is in between, so this is unclear.

*Changed to “Further studies revealed …”. (p. 2, l. 6)*

p. 2, l. 9: “comprehensive interpretation” -> review of PMSE physics?

*Changed.*

p. 2, l. 9: “Though, NLC..” Thus, NLC and PMSE are both indicators for..

*Changed.*

p. 2, l. 10: “indirect information on temperature … atmosphere where other data is sparse.”

*Changed.*

p. 3, l. 11: were grown, have grown?

*Changed.*

p. 3, l. 26: delete “daylight-capable”

*We prefer to keep this information, because daylight capability is essential for this study.*

p. 5, l. 25: “to allow for a radar backscatter signal”

*Phrasing without “for” was suggested by Reviewer 1 in first revision.*

# Simultaneous observations of NLC and MSE at midlatitudes: Implications for formation and advection of ice particles

Michael Gerding[1], Jochen Zöllner[1,*], Marius Zecha[1], Kathrin Baumgarten[1], Josef Höffner[1], Gunter Stober[1], and Franz-Josef Lübken[1]

[1]Leibniz-Institute of Atmospheric Physics at Rostock University, Kühlungsborn, Germany
[*]now at Planet AI GmbH, Rostock, Germany

*Correspondence to:* Michael Gerding (gerding@iap-kborn.de)

**Abstract.** ~~We have combined ground-based observations of ice particles in the summer mesopause region by lidar (then often called Noctilucent Clouds , NLC) and radar (then called (Polar)~~ We combined ground-based lidar observations of Noctilucent Clouds (NLC) with collocated, simultaneous radar observations of Mesospheric Summer Echoes ~~, (P)MSE) for a first comparative study on~~ (MSE) in order to compare ice cloud altitudes at ~~midlatitudes~~ a mid-latitude site (Kühlungsborn/Germany, 54° N, 12° E). Lidar observations are limited to larger particles (>10 nm), while radars are also sensitive to small particles (<10 nm), but require sufficient ionization and turbulence at the ice cloud altitudes~~to receive an echo. The combination of~~ . The combined lidar and radar ~~observations provides some rough information about~~ data set thus includes some information on the size distribution within the cloud and by this ~~about~~ on the 'history' of the cloud. The soundings for this study are carried out by the IAP RMR lidar and the OSWIN VHF radar. ~~We find a good agreement of~~ On average, there is no difference between the lower edges ($z^{\mathrm{low}}_{\mathrm{NLC}}$ and $z^{\mathrm{low}}_{\mathrm{MSE}}$)~~, showing a mean difference of only 40 m~~. The mean difference of the upper edges $z^{\mathrm{up}}_{\mathrm{NLC}}$ and $z^{\mathrm{up}}_{\mathrm{MSE}}$ is ∼500 m, which is much less than expected from observations at higher latitudes. In contrast to high latitudes, the MSE above our location typically do not ~~stretch~~ reach much higher than the NLC. In addition to earlier studies from our site, this gives additional evidence for the supposition that clouds containing large enough particles to be observed by lidar are not formed locally but are advected from higher latitudes. During the advection process, the smaller particles in the upper part of the cloud either grow and sediment, or they sublimate. Both processes result in a thinning of the layer. ~~Nucleation of new ice clouds (usually visible as high MSE) rarely happens at the same time as the NLC events~~High-altitude MSE, usually indicating nucleation of ice particles, are rarely observed in conjunction with lidar observations of NLC at Kühlungsborn.

## 1 Introduction

Noctilucent Clouds (NLC, also known as Polar Mesospheric Clouds, PMC) and Polar Mesospheric Summer Echoes (PMSE) have been observed since several decades mainly in the polar regions by ground-based and space-based instruments ~~as well as by human eye (e.g. Leslie, 1885; DeLand et al., 2003; Chu et al., 2003; Morris et al., 2007; Collins et al., 2009; Latteck and Bremer, 2017~~ ~~.~~ (e.g. DeLand et al., 2003; Chu et al., 2003; Morris et al., 2007; Collins et al., 2009; Latteck and Bremer, 2017). Even older data sets of NLC exist from visual observations (e.g. Leslie, 1885). Observations at mid latitudes showed that mesospheric ice

clouds can exist also equatorward of 60° latitude and occasionally even equatorward of 45° latitude (Thomas et al., 1994; Chilson et al., 1997; Wickwar et al., 2002; Ogawa et al., 2011; Russell et al., 2014). First simultaneous soundings of both phenomena have been achieved by Nussbaumer et al. (1996) at the ALOMAR observatory at 69° N. The observations stimulated the impression that both phenomena are related to ice clouds in the mesopause region, even if there are some differences in occurrence and vertical extension. NLC are usually observed between ∼80-86 km (e.g. Fiedler et al., 2017), while PMSE stretch higher and appear at ∼80-90 km (e.g. Latteck and Bremer, 2017). ~~Later on it was~~ Further studies revealed that PMSE additionally require sufficient ionization of the ambient air to get the ice particles charged. Additionally, scattering of the radar ~~happens~~ wave occurs only on structures in the plasma that are produced by turbulence but can persist even if the turbulence ceased. Rapp and Lübken (2004) published a ~~comprehensive interpretation of PMSE~~ review of PMSE physics and their relation to ice clouds in the mesopause region. ~~Though~~Thus, NLC and PMSE are both ~~an indicator~~ indicators for temperatures below the frost point, i.e. the ice clouds provide indirect ~~temperature information~~ information on temperature in a region of the atmosphere ~~,~~ where other data is sparse.

In this study we utilize combined observations by lidar and radar to gather information about the origin of the NLC layer at midlatitudes. There is some debate about the role of advection from higher latitudes compared to local ice particle formation. This is in particular important for the interpretation of trends in midlatitude ice clouds ~~that are used as an indicator for climate change in the middle atmosphere~~ (e.g. Thomas, 2003; Russell et al., 2014). Some studies found a strong dependence of ice observations on equatorward directed wind (Morris et al., 2007; Zeller et al., 2009; Gerding et al., 2013b) or planetary wave activity (Nielsen et al., 2011), while other studies explained the observations mainly by local temperature structure (e.g. Herron et al., 2007; Hultgren et al., 2011; Stevens et al., 2017). Simultaneous observations by lidar and radar give additional information on this topic due to their different size dependencies. Lidars are mainly sensitive to ice particles with diameters of some ten nanometers (NLC), while radar echoes ((P)MSE), ionization and turbulence provided, indicate small or large ice particles, where smaller particles may be freshly formed in the mesopause region and just start to sediment. Local NLC formation therefore implicates the simultaneous existence of freshly formed particles, i.e. of typically an MSE layer extending above the NLC. If the advection of NLC dominates, the initial ice particles should have already sedimented and grown.

Simultaneous observations of NLC and (P)MSE to solve this question are technically challenging and rare. They require a powerful lidar and a VHF radar being co-located. The lidar needs to be daylight-capable because (P)MSE are mainly limited to daylight conditions (e.g. Thomas et al., 1996; Zecha et al., 2003; Rapp and Lübken, 2004). During darkness and outside the auroral oval, the ionization in the D-region is typically too small to create radar echoes in the mesopause region. Additionally, the lidar needs to be sensitive enough for the typically weak NLC backscatter signals. So far, the only statistical studies on joint NLC and (P)MSE occurrence and layer parameters from simultaneous observations by lidar and radar are performed at polar latitudes (e.g. von Zahn and Bremer, 1999; Klekociuk et al., 2008; Kaifler et al., 2011). For most of the time of NLC detection also PMSE have been observed, while, on the contrary many PMSE have been detected in the absence of NLC. Typically, PMSE and NLC layers have very similar lower edges, but PMSE stretch several kilometers higher than NLC. Li et al. (2010) ~~revealed from~~ found in PMSE observations that average ice particle radii are smaller above 85 km than below. This can be explained by local ice formation in the high latitude mesopause region (observed as PMSE), happening in parallel

to the occurrence of larger ice particles below 85 km (observed as NLC and PMSE). These main layer properties are similar in northern and southern polar regions, even though observations at Davis (69° S) show typically less and weaker echoes compared to ALOMAR (69° N) (Morris et al., 2007; Latteck and Bremer, 2017). For midlatitudes, either only MSE or NLC statistics have been described so far. Midlatitude MSE layer properties have been published by Latteck et al. (1999) and Zecha et al. (2003) based on data of the OSWIN radar at Kühlungsborn (Germany, 54°N). They found a much lower occurrence rate compared to high latitudes in the Northern Hemisphere, but a similar altitude distribution. Midlatitude NLC layer properties have been described by Gerding et al. (2013a), using the Rayleigh-Mie-Raman lidar co-located with OSWIN. Similarly, they found a much smaller occurrence rate compared to high latitudes, but comparable NLC altitudes. Nevertheless, a joint examination of lidar and radar observations at our site is lacking.

In this paper we compare NLC and MSE layer properties such as lower and upper edges for all periods with simultaneous observations. By this we concentrate on events when at least part of the ice particles have ~~been~~ grown to sizes of some ten nanometers. By the combination of NLC and MSE signals we also avoid confusion of the ice-related MSE with other mesopheric echoes in summer that are sometimes observed at much lower latitudes, i.e. at much too high temperatures for ice existence (Muraoka et al., 1989; Kubo et al., 1997).

In the following Section 2 we describe the instrumentation and the available data set. The vertical distributions of layer edges and maxima are presented in Section 3. In Section 4 we examine the influence of local wind and temperature profiles on the ice NLC/MSE. In Section 5 we compare our results to data from polar latitudes, leading to our conclusion about the relevance of advection for NLC occurrence at our site.

## 2 Methodology and single layer comparison

The NLC and MSE observations used here are made at Kühlungsborn (54° N, 12° E) with the daylight-capable Rayleigh-Mie-Raman (RMR) lidar and the OSWIN VHF radar, respectively. Additional data are provided by the co-located potassium resonance lidar measuring temperatures above the NLC (e.g. von Zahn and Höffner, 1996; Alpers et al., 2004) and by the nearby (120 km to the north-east) meteor radar at Juliusruh (55° N, 13° E) (Stober et al., 2012, 2017). In this section we describe the main instruments, show some examples for edge detection and the general appearance of NLC and MSE, and give an overview on the used data and its representativeness.

### 2.1 NLC observations by the daylight-capable IAP RMR lidar at Kühlungsborn

The daylight-capable RMR lidar started operation in summer 2010 and replaced the former RMR lidar used for nighttime NLC observations. A general description of the lidar has been given by Gerding et al. (2016). In summary the lidar uses a frequency-doubled Nd:YAG laser at 532 nm with ∼20 W average power. The backscatter signal is collected by a single telescope of 80 cm diameter and detected by an Avalanche Photo Diode. The daylight capability is achieved by a field of view of the telescope of only ∼60 $\mu$rad, a narrow-band interference filter (130 pm), and a double Fabry-Pérot etalon (∼4 pm full spectral width at half maximum). The lidar is designed for observation of middle atmosphere temperatures and their variability due to gravity

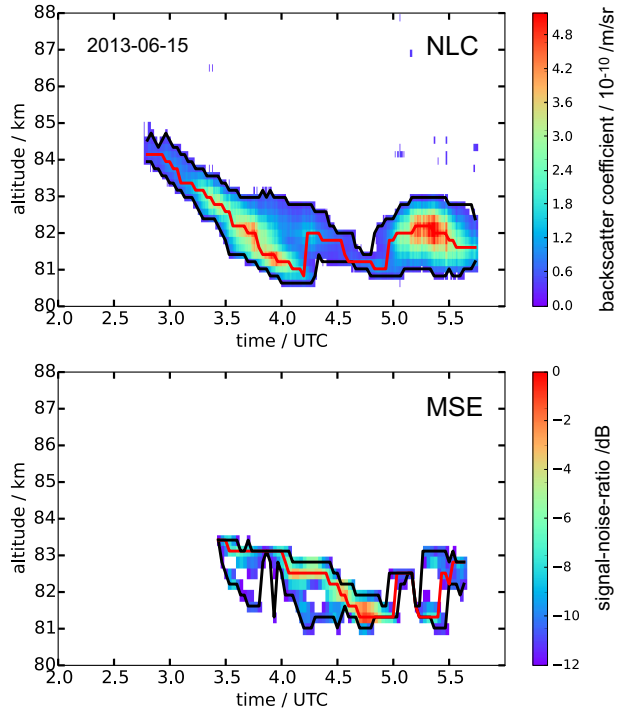


**Figure 1.** Examples for detection of NLC (top) and MSE (bottom) using observations on 15 June 2013. The black lines show the upper and lower edges ($z^{\mathrm{low}}$ and $z^{\mathrm{up}}$), the red line the layer maxima ($z^{\mathrm{max}}$). Edge detection is done on the temporal resolution of the radar (2 min). Edges are defined at $\beta = 0.3$ (NLC) and SNR = -12 dB (MSE).

waves and tides (Kopp et al., 2015; Baumgarten et al., 2018) and for detection of NLC in summer. For NLC measurements, aerosol and molecular scattering are separated by exponential interpolation of the background-corrected Rayleigh (molecular) backscatter signal above and below the cloud. The NLC backscatter coefficient at 532 nm ($\beta_{532}$) is then calculated from the aerosol backscatter normalized to the molecular backscatter, the molecular backscatter cross section, and a reference air density to quantify the cloud brightness. Under typical transmission conditions and during full daylight the sensitivity limit of the lidar for NLC is at $\beta_{532} = 0.3 \cdot 10^{-10}\,\mathrm{m^{-1}sr^{-1}}$ (in the following we describe $\beta_{532}$ in units of $10^{-10}\,\mathrm{m^{-1}sr^{-1}}$, i.e. here $\beta = 0.3$). For this study, the backscatter signal has been integrated for 30 s and smoothed by a running average over 15 min. The vertical resolution is set to 195 m. The individual profiles have been manually inspected for NLC and only positively identified profiles are used for further processing (cf. Gerding et al., 2013a). NLC backscatter maxima ($z^{\mathrm{max}}_{\mathrm{NLC}}$) and layer edges ($z^{\mathrm{low}}_{\mathrm{NLC}}$ and $z^{\mathrm{up}}_{\mathrm{NLC}}$) are evaluated automatically. A typical NLC case is shown in Figure 1 (upper panel). The layer edges, defined at $\beta = 0.3$, and layer maxima are identified by an algorithm and marked in the Figure by black and red lines.

**Fig.1**

### 2.2 MSE observations by the OSWIN VHF radar at Kühlungsborn

The monostatic OSWIN VHF radar (53.5 MHz) operated in an unattended and continuous measurement mode during the summer seasons. Until 2013 a phased-array antenna field consisting of 12 x 12 Yagi antennas was used. The beam could be tilted, but for the comparisons of MSE and NLC only the vertically directed beam with a beam width of 6° was selected. Two 16-bit complementary codes with 2 $\mu$s pulse elements were used. The repetition frequency was set to 1200 Hz. For reception, the antenna array was split in six subgroups with 24 antennas each, which were connected to six receivers. Data points were created by coherent integrations of 20 samples. Time series of 1024 data points are acquired within 34.1 s. Considering the time of further alternating measurements, the time resolution for MSE observations is 2 min. After 2013 the antenna array was refurbished. The new array is based on 133 Yagi antennas arranged in a hexagonal structure. The width of the vertically directed beam is about 6° again. Two 32-bit-complementary codes with 2 $\mu$s pulse elements and 625 Hz repetition frequency are used. For reception, six subgroups of 21 antennas each are connected to six receivers. Time series of 1024 samples (inclusive of eight coherent integrations) result in length of 26.2 s. In summary we assume fairly similar technical conditions regarding the radar measurements during the summer seasons. In both periods a height resolution of 300 m is maintained. The backscattered signals received by the six receivers are combined phase conform. Signal-to-noise ratios (SNR) are estimated from the autocorrelation functions of the time series in each height channel. As we do not have an absolute calibration of the radar, we use SNR as an approximation for the echo intensity. The lowest signal level used for MSE observations is chosen at an SNR of -12 dB. A typical example with identified edges is presented in Fig. 1 (lower panel).

### 2.3 Examples for simultaneous NLC-MSE observations

In the following we show different cases of simultaneous NLC-MSE observations to demonstrate the variability of the layers. Similar to previous studies we ~~partly find very large~~ often find very good agreement between NLC and MSE, while there are differences in other cases (cf. von Zahn and Bremer, 1999; Klekociuk et al., 2008; Kaifler et al., 2011). Examples are given in Figure 2 . Figure 2 a) shows an event that was observed on 17 June 2010. While the NLC (filled contours) was first detected above the limit of $\beta = 0.3$ at 2:45 UTC, the MSE (contour lines) was only observed after 3:30 UTC, when the solar elevation exceeded ∼5° and the ionization of the atmosphere was large enough to allow a radar backscatter signal. Then both phenomena follow the same vertical movement, presumably related to the cold phase of a gravity wave, with the MSE sometimes reaching to higher altitudes. **Fig.2**

Also on 10 July 2015 (Fig. 2 b) NLC and MSE showed a good agreement. The lidar was switched on at 13:50 UTC when the MSE already existed, and NLC were observed from the beginning of the lidar sounding, but in a smaller altitude range. Between 15:30 and 16:50 UTC the NLC vanished, but the MSE showed only a short gap of 10 min and set in again at a much higher altitude about half an hour before the NLC occurs again. Then both layers agreed well until the MSE disappeared at ∼19 UTC at a solar elevation of ∼4°. The NLC observation continued for another 5 h, until the layer descended below 80 km at 0 UTC.

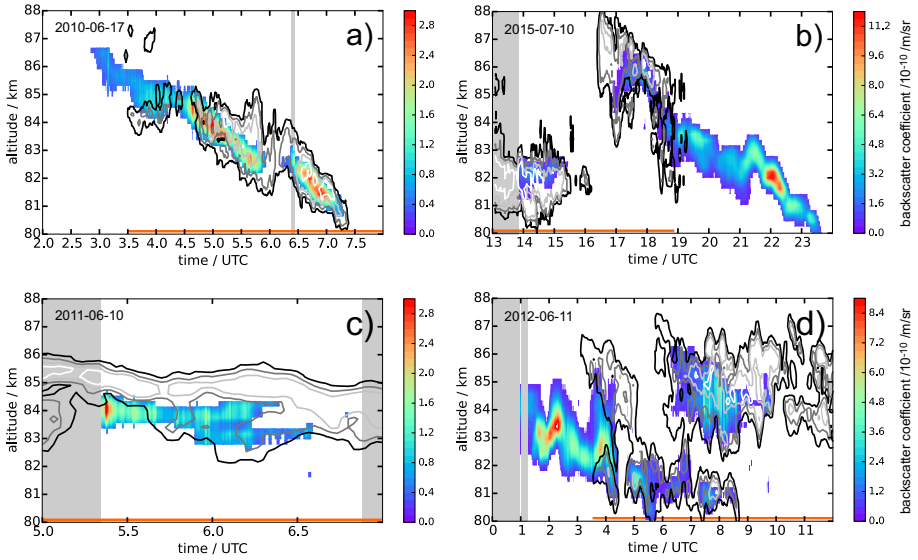


**Figure 2.** Examples for observations of MSE (contour lines at -12/-6/0/6 dB, if applicable) and NLC (filled contours with scale on the right). The orange lines indicate periods with solar elevation >5°. The gray shaded areas mark periods without lidar soundings due to presence of clouds. a) 17 June 2010: MSE starts after sunrise into existing NLC. b) 10 July 2015: MSE vanishes after sunset while NLC continuous. c) 10 June 2011: When lidar starts operation NLC is immediately detected, but does not extend as high as the MSE. d) 11 June 2012: MSE starts into existing NLC after sunrise and continues especially at higher altitudes when NLC disappears.

On 10 June 2011 (Fig. 2 c) NLC were observed from the beginning of the lidar sounding at 5:21 UTC. Earlier, the ice particles were already detected by the radar as MSE, but tropospheric clouds inhibited lidar operation. In contrast to the other cases, here ~~only the lower edges of the phenomena agreed, but the~~ the MSE extended above the NLC and was in fact strongest at altitudes above the NLC upper edge. Later on, the NLC ceased while the MSE continued.

A rare example of a double ice layer was observed on 11 June 2012 (Fig. 2 d). The cloud was first confirmed by the lidar, showing that the NLC was very variable in altitude due to the presence of gravity waves. After ∼3:20 UTC the NLC layer thickness increased to ∼5 km (81 – 86 km). Just at the same time the radar echo started due to increasing solar elevation, i.e. increasing ionization. The MSE quickly grew into a double layer, with a gap around 83 km altitude, where the NLC was found brightest. The NLC and MSE around 82 km faded away at 4:23 UTC and set in again at 4:40/4:45 UTC (MSE/NLC). In the meantime, the only remaining ice signal was observed by the radar above 83 km. Past ∼5 UTC the upper MSE layer vanished, but reappeared shortly after. At ∼6:15 UTC also the NLC formed a (very rare) double layer until ∼8:30 UTC, when the lower layer of both, NLC and MSE, ceased. Despite being weak, the upper NLC layer remained observable until ∼10 UTC, while the MSE still continued in a broad range (83 – 87 km). The variable structure of the ice cloud with double layers indicates a highly dynamic behavior of the atmosphere with presence of strong gravity waves. Nevertheless, a detailed examination of the dynamical structure is beyond the scope of this paper.

The examples shown above demonstrate the different relations of the NLC and MSE layer edges and the different degrees of accordance of the layers. This is in general agreement with observations at polar latitudes (e.g. Klekociuk et al., 2008; Kaifler et al., 2011). The examples indicate an often good concurrence of the lower edges but a worse agreement of the upper edges. If solar elevation (i.e. ionization) is sufficiently large, NLC are often but not always accompanied by MSE. The latter might be explained by the radar detection threshold or missing turbulence, but this cannot be ~~proven~~ checked here because a lack of appropriate measurements. Periods with MSE but absent NLC can be caused by mainly small ice particles, resulting in lidar signals below the NLC detection threshold. In the following we neglect profiles of NLC without MSE as well as MSE without NLC to be sure that for this study all requirements for the observation of small and large ice particles are fulfilled (see below).

### 2.4 The data set used for this study

Within this study we only focus on simultaneous NLC and MSE events (e.g., after 3:30 UTC in Fig. 2 a, but excluding the little MSE gaps between 4 – 5 UTC), to compare the altitude ranges where both phenomena are observed. Nighttime NLC, where ionization of the atmosphere is typically too small for MSE generation, are ignored as well as a few NLC where the radar was switched off for maintenance. Vice versa we do not count ice clouds (detected as MSE) that are found too weak to be observed by lidar or that occured when the lidar was switched off, e.g., during tropospheric cloud coverage. Overall, we use ~67 h of NLC with $\beta > 0.3$ for this study, out of 188.5 h of NLC in total ($\beta > 0$, day and night) in the years 2010 – 2016. ~~These data are distributed across 31 days with an average ice cloud duration of 2.2 h. For this study it is not relevant whether the ice observation is uninterrupted in time or not, because the layer parameters are derived based on individual (but smoothed) profiles.~~ About 121 h of NLC detection cannot be used here because of either too weak NLC ($\beta < 0.3$~~) or~~ , ~20%) or the absence of MSE~~(mainly missing ionization at night or missing turbulence).~~ . MSE get sparse at low solar elevation, because of missing ionization (~35% of the time the solar elevation is below 5°). Furthermore, either turbulence can be missing or the radar detection threshold can be too high. Nevertheless, this subset of NLC is representative for the whole data set in terms of layer heights, as discussed in Section 5. The total usable lidar operation time within the seven summers (1 June to 4 August) is 3337 h. MSE are observed by OSWIN for 960 h out of 8600 h of total sounding time. As mentioned above, only for 67 h the MSE (SNR > 12 dB) occur during lidar operation and simultaneously with NLC of $\beta > 0.3$. These data are distributed across 31 days with an average ice cloud duration of 2.2 h. For this study it is not relevant whether the ice observation is uninterrupted in time or not, because the layer parameters are derived based on individual (but smoothed) profiles. Note that this study is representative for ice clouds containing sufficiently large particles to be detectable by lidar, but it is not representative for MSE (ice clouds) in general.

## 3 Comparison of NLC and MSE layer properties

Based on the data set of simultaneous NLC and MSE (gridded to 2 min temporal resolution) we identify the lower edges ($z^{\mathrm{low}}_{\mathrm{NLC}}$ and $z^{\mathrm{low}}_{\mathrm{MSE}}$), the altitudes of maximum brightness ($z^{\mathrm{max}}_{\mathrm{NLC}}$ and $z^{\mathrm{max}}_{\mathrm{MSE}}$) and the upper edges ($z^{\mathrm{up}}_{\mathrm{NLC}}$ and $z^{\mathrm{up}}_{\mathrm{MSE}}$) for each profile of both phenomena independently, as shown in Fig. 1. In the rare case of a double layer we take the lower edge of the lower

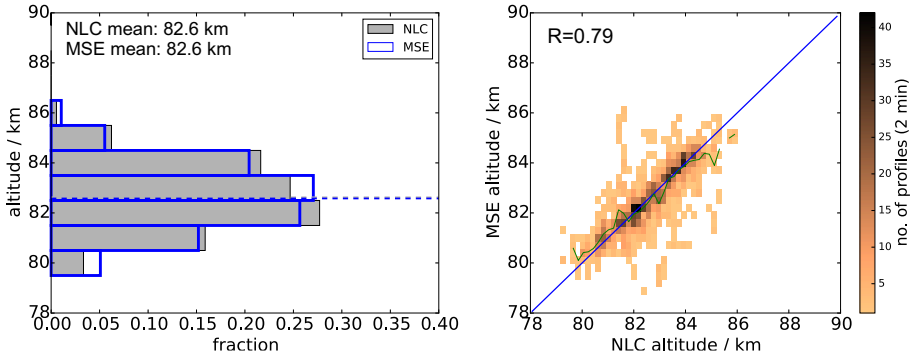


**Figure 3.** Comparison of lower edges of NLC and MSE ($z^{\mathrm{low}}_{\mathrm{NLC}}$ and $z^{\mathrm{low}}_{\mathrm{MSE}}$). a) Histogram with NLC edges in grey (filled) and MSE edges in blue (open histogram). Mean values are indicated by the dashed lines. b) Scatter plot of MSE and NLC edges. Only simultaneous soundings based on a 2 minute temporal resolution are evaluated. The green line in b) shows the average MSE lower edge altitude for each NLC edge bin and the blue line indicates identical altitudes.

layer and the upper edge of the upper layer together with the absolute maximum. Overall, we get 1931 profiles with their respective properties, even if the particular smoothing of lidar and radar data needs to be taken into account for interpretation. In Figure 3 (left) the altitude distributions of $z^{\mathrm{low}}_{\mathrm{NLC}}$ and $z^{\mathrm{low}}_{\mathrm{MSE}}$ are summarized in 1 km bins. The most striking feature is the **Fig.3** similarity between the altitude distributions of NLC and MSE lower edges. In the evaluated data set, no cloud is observed below 80 km. The mean values of both, $z^{\mathrm{low}}_{\mathrm{NLC}}$ and $z^{\mathrm{low}}_{\mathrm{MSE}}$ are found at ∼82.6 km (dashed lines). The figure shows only small differences between both distributions. In Figure 3 (right) the lower edges of all individual NLC/MSE profiles are compared. The plot confirms the similarity between both parameters. Most often the $z^{\mathrm{low}}$ agree within a single altitude bin, which also shows up in the correlation coefficient of R=0.79. The differences between $z^{\mathrm{low}}_{\mathrm{NLC}}$ and $z^{\mathrm{low}}_{\mathrm{MSE}}$ can be up to a few hundred meters, and there is no altitude dependence of the differences. Thus, very high ice clouds show the same similarity as low or typical layers. The mean difference between $z^{\mathrm{low}}_{\mathrm{NLC}}$ and $z^{\mathrm{low}}_{\mathrm{MSE}}$ is ∼40 m with a standard deviation of 417 m. In a few cases the altitude difference can be up to 4 – 5 km. This can already be seen in Fig. 2 d), e.g., in cases of MSE onset in the morning twilight where sometimes the MSE only agrees with the uppermost part (i.e. largest ionization) of the ice cloud. Part of the differences can also be explained by the different fields of view (FOV). The radar has a FOV of 6° = 0.1 rad, while the lidar FOV is only ∼1/1700 of this (62 $\mu$rad). This may lead to some differences at least in cases of very structured ice clouds~~.~~, because any feature in the ice cloud needs some time for drifting through the radar FOV, e.g. ∼3.5 min at 20 m/s wind speed. Rarely, the different size dependencies of lidar and radar signals can lead to MSE even a few km below the NLC. On average, these effects only have a small influence on the general distribution.

The altitude distribution of the ice layer maxima (backscatter coefficient for NLC and signal-to-noise ratio for MSE) is shown in Figure 4 . The mean of $z^{\mathrm{max}}_{\mathrm{NLC}}$ is observed at 83.3 km (grey dashed line in left panel), while the mean of $z^{\mathrm{max}}_{\mathrm{MSE}}$ is slightly **Fig.4** higher at 83.6 km (blue dashed line in left panel). No NLC maximum is observed above 86 km, but a few MSE maxima. This is also resembled in the scatter plot (Fig. 4, right). Similar to the lower edges there is no pronounced altitude dependence of

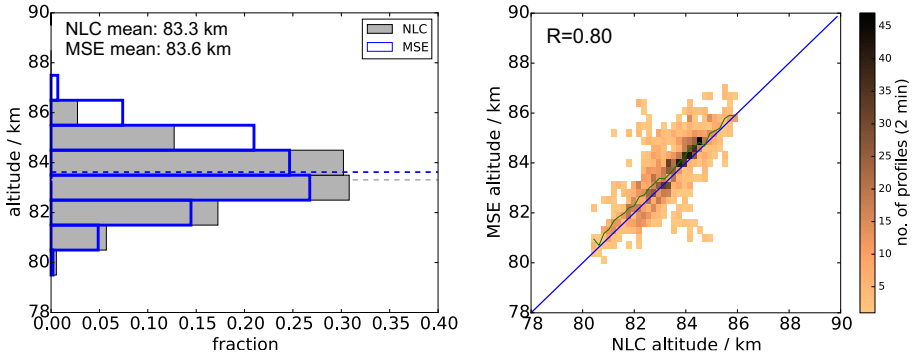


**Figure 4.** Same as Figure 3, but for the layer maxima ($z^{\max}_{\mathrm{NLC}}$ and $z^{\max}_{\mathrm{MSE}}$).

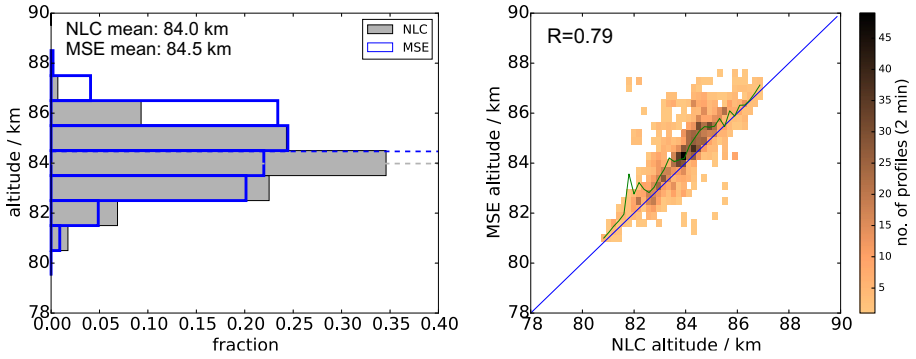


**Figure 5.** Same as Figure 3, but for the upper edges of NLC and MSE ($z^{\mathrm{up}}_{\mathrm{NLC}}$ and $z^{\mathrm{up}}_{\mathrm{MSE}}$).

the differences between $z^{\max}_{\mathrm{NLC}}$ and $z^{\max}_{\mathrm{MSE}}$ (green line). The correlation coefficient is R=0.80. While again the individual $z^{\max}_{\mathrm{NLC}}$ and $z^{\max}_{\mathrm{MSE}}$ sometimes differ by a few kilometers, the mean value of the differences is only ∼300 m with a standard deviation of 375 m.

The largest differences between NLC and MSE are expected at the upper edges of the layer (cf. Kaifler et al., 2011). This is due to the fact that the nucleation typically starts close to the mesopause, where water vapour saturation is largest. These small particles can already be detected by radars (signal strength proportional $r^2$, if turbulence and ionization allow). If the supersaturated region extends further down, the particles start to sediment and grow, and become finally visible for lidars (signal strength proportional $r^5..r^6$). Indeed, we find the mean $z^{\mathrm{up}}_{\mathrm{MSE}}$ about 500 m above the mean $z^{\mathrm{up}}_{\mathrm{NLC}}$ for all simultaneous observations (Figure 5 ), i.e. at 84.5 km and 84.0 km, respectively. The scatter plot shows that the height difference is largely independent of altitude. Only for the very high (>85 km) and very low (<82 km) layers the differences seem to vanish, but the number of such events is small. The smaller height difference can be explained by the typically smaller width of the ice clouds at these altitudes (not shown). In contrast to the layer maxima and lower edges, differences of a few kilometers are mainly found with the MSE top being much higher than the NLC top. Thus, the distribution of differences is not symmetric, but has a tail towards higher MSE as typically expected. Note that the correlation of $z^{\mathrm{up}}_{\mathrm{MSE}}$ and $z^{\mathrm{up}}_{\mathrm{NLC}}$ is still high (R=0.79).

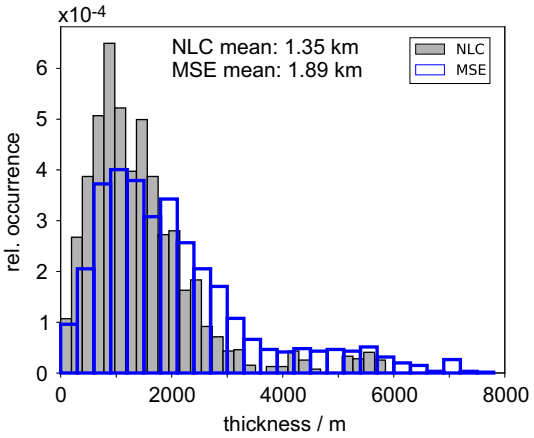


**Figure 6.** Histogram of layer thicknesses, calculated as $z^{\mathrm{up}}_{\mathrm{NLC}} - z^{\mathrm{low}}_{\mathrm{NLC}}$ for NLC (grey, filled) and $z^{\mathrm{up}}_{\mathrm{MSE}} - z^{\mathrm{low}}_{\mathrm{MSE}}$ for MSE (blue, open). The relative occurrence (O) is normalized such that all bins times the bin width ($\Delta$) sum to 1, i.e. $\sum (O \cdot \Delta) = 1$. Bin widths are 195 m for NLC and 300 m for MSE.

From the upper and lower edges the NLC and MSE layer thicknesses can easily be calculated. The results are shown in the histograms in Figure 6 . Typically, the NLC thickness ($z^{\mathrm{up}}_{\mathrm{NLC}} - z^{\mathrm{low}}_{\mathrm{NLC}}$) is below 2 km, with a mean value of 1.35 km. The MSE are typically slightly thicker, having a mean layer thickness of 1.89 km. These numbers are already expected from the difference of mean upper and lower edges. Furthermore, the histogram shows a larger quantity of thick MSE, having thicknesses of more than 4 km. That means that in a few cases the MSE width is much larger than the NLC width, but the average layer thicknesses differ by only ∼500 m. **Fig.6**

## 4 Comparison of NLC/MSE with local wind and temperature structure

There is general agreement that ice clouds are limited to regions with temperatures below the frost point temperature. For our location we have already shown that NLC occur only in the cold phases of gravity and planetary waves, while mean temperatures are above the frost point in the whole mesopause region (Gerding et al., 2007, 2013a). Additionally, we demonstrated that southward directed winds are necessary for the occurrence of NLC at our site (Gerding et al., 2007, 2013b). Here we want to check whether the ambient wind and temperature conditions are responsible for the altitude of the layer edges, i.e. the thickness of the NLC and MSE. We therefore evaluated the temperatures and winds especially above the layers.

Temperature soundings above MSE require a metal resonance lidar (for the altitude coverage) and daylight capabilities (for observation during MSE). The potassium resonance lidar at Kühlungsborn was in operation until the end of 2012, i.e. it covered part of the examined time period. The upper panel of Figure 7 shows an example of the temperature structure above two ice layers in the early morning of 27 June 2011. The first layer ('Cloud 1') arose at ∼2:30 UTC in the lidar (NLC, coloured layer) and did not extend above 83.5 km. The MSE (grey contour lines) appeared first at 3:30 UTC in 84.3 km, when ionization was sufficient (solar elevation 4.7°). Above Cloud 1 the potassium resonance lidar observed temperatures of more than 150 K, **Fig.7**

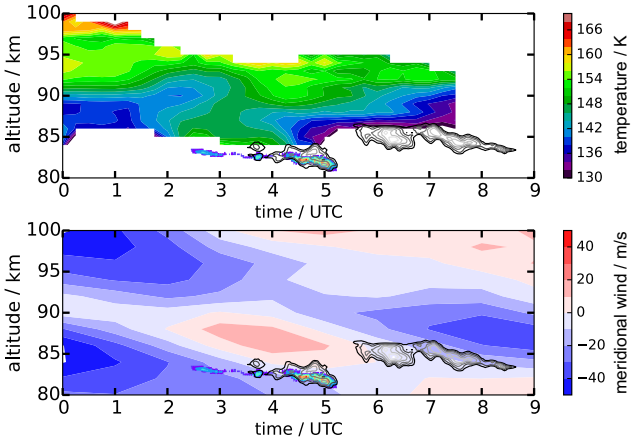


**Figure 7.** Temperature (top) and meridional wind (bottom) above Kühlungsborn during 26/27 June 2011. The MSE data is embedded in both panels for illustration as open grey contours and the NLC data in colored filled contours. Cloud 1: 2:30 – 5:15 UTC, Cloud 2: 5:30 – 8:40 UTC

i.e. higher than the expected frost point temperature for these altitudes. In other words, the temperature structure inhibits an expansion of the layer to higher altitudes. Later, Cloud 1 descends and vanishes at 5:15 UTC. Another ice layer ('Cloud 2') appeared at ∼5:30 UTC around 86 km. This coincides with a strong temperature decrease below ∼140 K in the same altitude range. We point out that Cloud 2 was observed by radar only (MSE), but did not contain particles large enough to be observed by lidar (NLC). Lidar observations stopped due to tropospheric clouds at ∼8 UTC. Note the integration time of the temperature data of 2 h, shortened to 1 h at the beginning and end of the sounding.

The lower panel of Fig. 7 shows the meridional wind observed by the nearby meteor radar (120 km north-east of Kühlungsborn). The warm region above Cloud 1 is accompanied by a northward wind, while the wind in the altitude of the layer is southward as expected from previous observations. At the time and altitude of the (higher) Cloud 2 the wind direction has changed to a weak southward wind. Overall, this typical case shows a large likelihood for advection of Cloud 1 that appeared as both MSE and NLC, because local ice formation is inhibited by the high temperatures above 85 km. Note that before 02 UTC low temperatures of ∼140 K have been observed above 85 km, but at this time no ice cloud was observed. The second case (Cloud 2) has the potential for local formation above 85 km, but this layer is confined to higher altitudes and does not contain larger ice particles (NLC). Both clouds are confined to southward winds.

We have analysed the temperature and wind data set above the NLC/MSE for all available coincident measurements. Due to often hazy sky conditions and therefore large solar background at near-infrared wavelengths, the temperature data set of the potassium lidar is smaller than the NLC data set of the RMR lidar. Between 2010 and 2012 only seven events can be evaluated, with some of the data sets showing a gap of up to 2 km between the NLC/MSE and the temperature data. The temperature structure above the ice clouds varies between the events. Partly, we find an immediate temperature increase above (five cases), inhibiting ice existence in these heights. In the other two cases, the supersaturated region extends for some kilometers above the observed ice cloud and includes the height region expected for nucleation (87 – 90 km, e.g. Kiliani et al. (2013)). In this case,

ice particles may still exist in the supersaturated region, even if not detected by the OSWIN radar. Low temperatures typically persist only for a few hours at our site (e.g. Gerding et al., 2007). In this time, ice particles only grow to a few nanometers radius (Rapp and Thomas, 2006), and continuous turbulence is needed to create radar echoes, in contrast to intermittent turbulence being sufficient in combination with larger ice particles (Rapp and Lübken, 2004). Additional ionization is needed in both cases. Unfortunately, there is no information about ambient turbulence available and the question about ice existence cannot be finally answered.

The wind structure above the NLC/MSE is also not uniform in all events. Overall, 23 events between 2010 and 2016 have been evaluated. During most of the events (nine cases) the wind above the ice layer is southward (as in the ice layer). Seven cases show northward winds above the cloud. In three cases the wind direction is changing, while four cases show only weak winds (less than $\pm 10$ m/s).

## 5 Discussion

Studies on the layer properties of NLC and MSE at midlatitudes are rare, because there is only a small occurrence frequency of 5 – 10% for MSE and NLC (e.g. Thomas et al., 1996; Zecha et al., 2003; Gerding et al., 2013a). Therefore, analyses of average layer parameters need multi-year observations to yield a representative data base. The only statistical NLC study at midlatitudes has been done at our site at Kühlungsborn based on the nighttime observations of the previous RMR lidar (Gerding et al., 2013a). The results are in good agreement with the data presented here. They report a mean centroid height of 82.7 km which compares very well with the mean centroid height of 82.6 km and mean peak height of 82.8 km of all NLC (daytime and nighttime) in the 2010–2016 period used here. Selecting only days that also show MSE, the mean NLC peak height is slightly higher (83.0 km), but within the geophysical variability. The remaining difference to the mean $z_{\mathrm{NLC}}^{\mathrm{max}}$ of 83.3 km mentioned in Fig. 4 can be explained by the further selection of profiles really showing simultaneous MSE. Especially some very low NLC profiles (below 80 km) are excluded here because of missing MSE, which is potentially caused by the reduced electron density. Furthermore, the faintest NLC profiles with $\beta < 0.3$, e.g., in the beginning and end of events are also excluded in Fig. 4. Therefore the apparent difference in NLC layer heights compared to previous studies can be explained by geophysical variability and treatment of the NLC data. But this does not hamper the representativeness of this study for all NLC.

For MSE there is an earlier study by Zecha et al. (2003) using radar data from Kühlungsborn. They report the occurrence rate of MSE at each particular height bin which is different from the histogram of peak altitudes that we present here. Even more important, we limit the MSE data set to events with simultaneous NLC, because we want to focus on optically visible ice clouds. By this we suppress weak and high (typically $>$86 km) layers of MSE that are often not accompanied with NLC. We note that we skip the majority of MSE by this selection. Therefore, the results presented here are not representative for all MSE.

As explained above, there are only very few studies for high-latitude, simultaneous NLC and PMSE. Kaifler et al. (2011) evaluated a large data set of NLC and PMSE from ALOMAR (69° N, 16° E). Simultaneous events are summarized in their categories III, IV, and V. In their Table 3 they report also quasi-identical lower edges of NLC and PMSE, even if the $z^{\mathrm{low}}$ at

higher latitudes are observed 0.5 km ~~above~~ below the midlatitude values. ~~This latitudinal difference of $z^{\mathrm{low}}$ can be explained by the general increase of NLC altitudes with latitude (Lübken et al., 2008; Chu et al., 2011) which is related to the ambient temperature structure~~The identity of NLC and MSE lower edges is to some extend induced by the data selection criteria. Kaifler et al. (2011) used only NLC with a peak brightness of $\beta > 4$, shifting the lower edge a few hundred meters down compared to all NLC (their Fig. 5). We find a similar effect in our data set (not shown). This explains, together with the fact that NLC are thinner at midlatitudes, the altitude difference of NLC lower edges between high and midlatitudes.

Regarding the upper edges ($z^{\mathrm{up}}_{\mathrm{NLC}}$ and $z^{\mathrm{up}}_{\mathrm{PMSE}}$), Kaifler et al. (2011) report a mean difference of ∼3.3 km, i.e. much larger than the difference of 0.5 km that we observe at midlatitudes. Klekociuk et al. (2008) examined one season of simultaneous observations of NLC and PMSE at 69° S at Davis Station (Antarctica). Occurrence rates of both phenomena are much smaller compared to the Northern Hemisphere. The authors do not provide numbers for the upper and lower edges of the layers, but from their Fig. 1 one can expect a difference of the upper edges similar to the numbers given by Kaifler et al. (2011). We therefore examined whether the small difference $z^{\mathrm{up}}_{\mathrm{MSE}} - z^{\mathrm{up}}_{\mathrm{NLC}}$ presented here is an arbitrary result of our limited data set. We chose different sub-data sets containing about half of the profiles, either by a random process or by selecting only the first or second half of the data. The small difference of upper edges persisted throughout all selection runs, varying between 0.2 km and 0.7 km.

The reason for the large height difference between $z^{\mathrm{up}}_{\mathrm{NLC}}$ and ~~$z^{\mathrm{up}}_{\mathrm{MSE}}$~~ ~~$z^{\mathrm{up}}_{\mathrm{PMSE}}$~~ at high latitudes is the typically much larger thickness of the PMSE layer ~~(cf. Kaifler et al., 2011).~~ (cf. our Fig. 6 and Table 3 in Kaifler et al. (2011)). In agreement with these observations, Kiliani et al. (2013) demonstrated with a 3d trajectory model the formation of ice-particles at the high-latitude mesopause, and subsequent descent and growth. At high latitudes often a layer of small particles (only visible by radar) exists above the larger ice particles that can also be detected by lidar. This situation is in qualitative agreement ~~mit~~ with Odin/OSIRIS observations (Hultgren and Gumbel, 2014) and sketched in the upper part of Figure 8 . The small difference between upper layer edges in our observations suggests that the layer of small particles is missing at midlatitudes. In this case, the larger, optically visible ice particles cannot be formed locally, but typically have to be advected (see lower left part of Fig. 8). Kiliani et al. (2013) found in their simulations the last ∼6 h before observation being most relevant for particle growth. In this period, the ice particles typically travel 150–500 km southward. Before, the ice particles remained small (< 20 nm) for more than 60 h. In agreement with this, NLC above Kühlungsborn are generally observed during southward wind conditions (Gerding et al., 2007, 2013a, b), and also in the Southern Hemisphere NLC even at high latitudes (69° S) are typically limited to equatorward winds (Morris et al., 2007; Klekociuk et al., 2008). In contrast, Stevens et al. (2017) found a dominating dependence of NLC on local temperatures even at midlatitudes, using NOGAPS-ALPHA assimilated model data. The authors explicitly neglected transport effects by using a 0-D NLC model, making a direct comparison with our findings difficult. Similarly, Herron et al. (2007) and Hultgren et al. (2011) found local effects dominating the formation of NLC for their midlatitude observations.

**Fig.8**

Furthermore, we cannot exclude longitudinal differences for the formation of ice clouds. According to SOFIE observations our site is at the longitude of minimal NLC occurrence rates (Hervig et al., 2016), suggesting different cloud formation mechanisms compared to other longitudes. It has been shown before for our site that temperatures below the frost point as

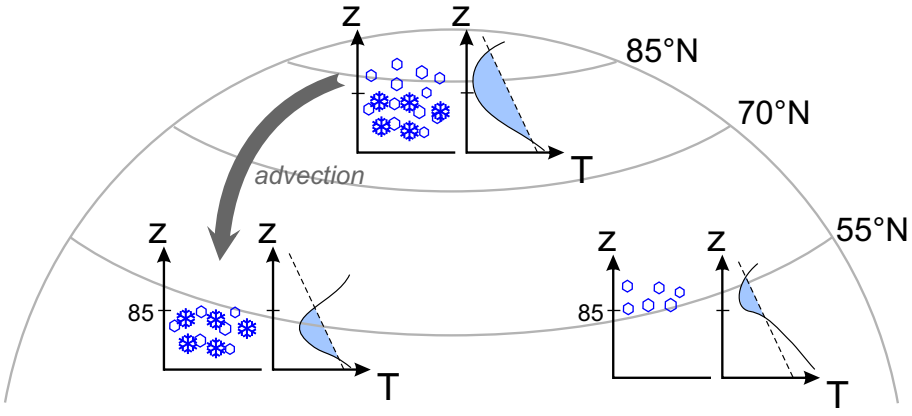


**Figure 8.** Schematic of the latitudinal differences for ice cloud formation. The x-y-plots represent the ice particle distribution with height (left) and the corresponding temperature profile (right). Small particles only visible for the radar are marked by light blue hexagons, larger particles by blue snowflakes. The light blue part of the temperature profile shows the region of supersaturation (dashed: frost-point temperature). The altitude of 85 km is marked, forming a typical upper limit of NLC.

well as southward winds are necessary but not sufficient criteria for NLC observations (Gerding et al., 2007). Supersaturated regions upstream of Kühlungsborn are needed to foster the nucleation process and to allow for the particles to grow to sufficient sizes (Fig. 8, lower left). About one third of the events examined here show southward winds also above the layer. The fact that these air parcels do not contain ice particles again confirms that southward winds are necessary but not sufficient for ice existence above our site. On the other hand, in another third of our events we found northward winds directly above the cloud, i.e. advecting air from (presumably) warmer regions. We would like to note that the OSWIN radar often detects MSE in thin layers above 85 km altitude (e.g. Zecha et al., 2003). We cannot exclude that these MSE are formed by ice particles nucleated closeby. But these particles typically do not reside long enough at our site to grow to sizes that allow optical detection, or the supersaturated height range is too thin to allow effective growth during sedimentation. This is sketched in the lower right part of Fig. 8.

In contrast to the upper edges, the lower edges of NLC and PMSE at 69° N typically agree quite well (Kaifler et al., 2011), similar to our observations. This is in fact expected due to the fast sublimation of the ice particles with typically rising temperatures at the lower edge of the layer. Of course, the instrument's sensitivity needs to be taken into account for comparison of layer edges. For the lidar observations described here we set the threshold to $\beta = 0.3$, which is slightly smaller than the threshold used in Gerding et al. (2013b) for the same lidar ($\beta = 0.5$). We confirmed by manual inspection that the edges of the individual NLC are correctly identified and not affected by background noise. For the radar data we processed the data in units of SNR. The threshold is set to -12 dB to be above the typical noise limit of the radar. We tested the influence of this threshold by setting it to larger and smaller numbers. Figure 9 shows the same histogram as Fig. 5, but for thresholds of -10 dB and -14 dB. As expected, the mean $z_{\mathrm{MSE}}^{\mathrm{up}}$ rises to 84.6 km if also weaker MSE are included. Limiting the data to >-10 dB, we found the mean $z_{\mathrm{MSE}}^{\mathrm{up}}$ at 84.4 km. In other words, the mean shift between both test scenarios is only 200 m, i.e. less than one

**Fig.9**

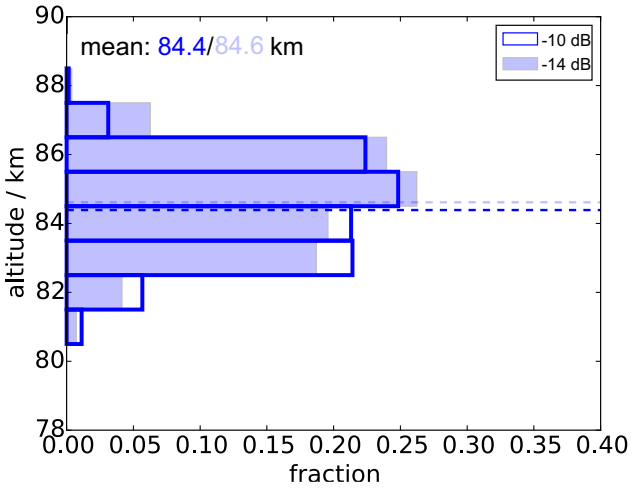


**Figure 9.** Same as Figure 5, but with different MSE thresholds. blue, open: MSE threshold SNR = -10 dB; light blue filled: MSE threshold SNR = -14 dB.

altitude bin of the radar (300 m). Changing the NLC threshold has similar results. Also here the gradients at the layer edges are very large (see, e.g., Fig. 2) and a change of the threshold to, e.g., $\beta = 0.5$ would result in only minor changes of the histograms. Therefore, there are only minor effects of the thresholds on layer edges, while the layer maximum is not affected at all. In any case, the changes due to threshold adaptions are much smaller than the difference to observations at higher latitudes.

## 6 Summary and Conclusions

In this study we compared NLC and MSE altitudes from simultaneous observations at our midlatitude site Kühlungsborn (54° N, 12° E). There is general agreement that both phenomena represent ice clouds, with the visible echoes (NLC) being formed by ice particles of typically some tens of nanometers diameter. The radar echoes (MSE) can also be formed by smaller particles, but require a sufficient density of free electrons as well as structures in the plasma. We have presented examples for NLC-only and MSE-only periods as well as for simultaneous layers with at least partial overlap in the covered altitude region. For the average layer parameters we only concentrated on simultaneous detections, i.e. we discarded nighttime NLC because of typically too small electron densities to form MSE. Furthermore we discarded all those high and weak MSE that are not accompanied with NLC. Overall, we got ∼67 h of NLC/MSE data within the summers 2010 – 2016.

On average, the lower edges of NLC and MSE are identical, which is in agreement with the general understanding of quickly sublimating ice particles at the bottom of the layer. The average values for the layer peaks and for the upper edges differ by 0.3 km and 0.5 km, respectively, with the MSE being slightly above the NLC. This comparatively small difference is in contrast to the observations at polar latitudes, where the PMSE often extend several kilometers above the NLC. We ~~conclude that the layer~~ found that the ice cloud itself is much thinner compared to polar latitudes (under the assumption that the MSE layer thickness at midlatitudes is not limited by smaller electron density or missing turbulence). Clouds that already exist long

enough to form large particles (NLC) show only a thin layer of small particles (invisible for the lidar but visible as MSE) above the NLC ~~or no such layer at all , at our site.~~at our site. Or they show no particles at all above the NLC, i.e. the upper edges of NLC and MSE coincide. Using simultaneous resonance lidar temperature soundings we typically found the atmosphere above the layer being too warm for ice existence, limiting the potential extent of the cloud. Meridional winds above the NLC ~~are often southward or weak~~do not show a preferential direction for the examined events. Altogether, these observations give evidence that local formation of ~~NLC/~~MSE is possible, but these ice particles do not stay long enough to grow to optically visible sizes. All layers that are observed as NLC are already formed and then advected to our site by the meridional wind. During advection and descent, the smaller particles grow to sizes of some ten nanometers. By this, they become detectable by lidar. This formation process must be taken into account if, e.g., midlatitude NLC observations are used to study trends or climate change in the mesopause region.

*Competing interests.* The authors declare that they have no conflict of interest.

*Acknowledgements.* We thank our colleagues Torsten Köpnick, Reik Ostermann, Michael Priester and Jörg Trautner for their support in lidar and radar operation and maintenance. We acknowledge the contributions of numerous students helping with continuous lidar soundings. Part of this work was supported by the Deutsche Forschungsgemeinschaft (DFG) under grant GE 1625/2-1. We thank the reviewers for their valuable comments that improved the manuscript. Presented data are available at ftp://ftp.iap-kborn.de/data-in-publications/ GerdingACP2018/.

## References


Alpers, M., Eixmann, R., Fricke-Begemann, C., Gerding, M., and Höffner, J.: Temperature lidar measurements from 1 to 105 km altitude using resonance, Rayleigh, and rotational Raman scattering, Atmos. Chem. Phys., 4, 793–800, 2004.

Baumgarten, K., Gerding, M., Baumgarten, G., and Lübken, F.-J.: Temporal variability of tidal and gravity waves during a record long 10 day continuous lidar sounding, Atmospheric Chemistry and Physics, 18, 371–384, https://doi.org/10.5194/acp-18-371-2018, https://doi.org/10.5194/acp-18-371-2018, 2018.

Chilson, P. B., Czechowsky, P., Klostermeyer, J., Rüster, R., and Schmidt, G.: An investigation of measured temperature profiles and VHF mesosphere summer echoes at midlatitudes, J. Geophys. Res., 102, 23 819–23 828, https://doi.org/10.1029/97JD01572, 1997.

Chu, X., Gardner, C. S., and Roble, R. G.: Lidar studies of interannual, seasonal, and diurnal variations of polar mesospheric clouds at the South Pole, J. Geophys. Res., 108, 8447, https://doi.org/10.1029/2002JD002524, 2003.

Chu, X., Huang, W., Fong, W., Yu, Z., Wang, Z., Smith, J. A., and Gardner, C. S.: First lidar observations of polar mesospheric clouds and Fe temperatures at McMurdo (77.8°S, 166.7°E), Antarctica, Geophys. Res. Lett., 38, L16810, https://doi.org/10.1029/2011GL048373, 2011.

Collins, R., Taylor, M., Nielsen, K., Mizutani, K., Murayama, Y., Sakanoi, K., and DeLand, M.: Noctilucent cloud in the western Arctic in 2005: Simultaneous lidar and camera observations and analysis, J. Atmos. Solar-Terr. Phys., 71, 446 – 452, https://doi.org/10.1016/j.jastp.2008.09.044, 2009.

DeLand, M. T., Shettle, E. P., Thomas, G. E., and Olivero, J. J.: Solar backscattered ultraviolett (SBUV) observations of polar mesospheric clouds (PMCs) over two solar cycles, J. Geophys. Res., 108, 8445, https://doi.org/10.1029/2002JD002398, 2003.

Fiedler, J., Baumgarten, G., Berger, U., and Lübken, F.-J.: Long-Term Variations of Noctilucent Clouds at ALOMAR, J. Atmos. Solar-Terr. Phys., 162, 79–89, https://doi.org/10.1016/j.jastp.2016.08.006, 2017.

Gerding, M., Höffner, J., Rauthe, M., Singer, W., Zecha, M., and Lübken, F.-J.: Simultaneous observation of NLC, MSE and temperature at a midlatitude station (54°N), J. Geophys. Res., 112, D12111, https://doi.org/10.1029/2006JD008135, 2007.

Gerding, M., Höffner, J., Hoffmann, P., Kopp, M., and Lübken, F.-J.: Noctilucent Cloud variability and mean parameters from 15 years of lidar observations at a mid-latitude site (54°N, 12°E), J. Geophys. Res., 118, 317–328, https://doi.org/10.1029/2012JD018319, 2013a.

Gerding, M., Kopp, M., Hoffmann, P., Höffner, J., and Lübken, F.-J.: Diurnal variations of midlatitude NLC parameters observed by daylight-capable lidar and their relation to ambient parameters, Geophys. Res. Lett., 40, 6390–6394, https://doi.org/10.1002/2013GL057955, 2013b.

Gerding, M., Kopp, M., Höffner, J., Baumgarten, K., and Lübken, F.-J.: Mesospheric temperature soundings with the new, daylight-capable IAP RMR lidar, Atmos. Meas. Tech., 9, 3707–3715, https://doi.org/10.5194/amt-9-3707-2016, http://www.atmos-meas-tech.net/9/3707/2016/, 2016.

Herron, J. P., Wickwar, V. B., Espy, P. J., and Meriwether, J. W.: Observations of a noctilucent cloud above Logan, Utah (41.7° N, 111.8° W) in 1995, J. Geophys. Res., 112, D19203, https://doi.org/10.1029/2006JD007158, 2007.

Hervig, M. E., Gerding, M., Stevens, M. H., Stockwell, R., Bailey, S. M., Russell III, J. M., and Stober, G.: Mid-latitude mesospheric clouds and their environment from SOFIE, J. Atmos. Solar-Terr. Phys., 149, 1–14, https://doi.org/10.1016/j.jastp.2016.09.004, 2016.

Hultgren, K. and Gumbel, J.: Tomographic and spectral views on the lifecycle of polar mesospheric clouds from Odin/OSIRIS, J. Geophys. Res., 119, 14,129–14,143, https://doi.org/10.1002/2014JD022435, 2014.

Hultgren, K., Körnich, H., Gumbel, J., Gerding, M., Hoffmann, P., Lossow, S., and Megner, L.: What caused the exceptional mid-latitudinal noctilucent cloud event in July 2009, J. Atmos. Solar-Terr. Phys., 73, 2011.

Kaifler, N., Baumgarten, G., Fiedler, J., Latteck, R., Lübken, F.-J., and Rapp, M.: Coincident measurements of PMSE and NLC above ALOMAR (69° N, 16° E) by radar and lidar from 1999–2008, Atmos. Chem. Phys., 11, 1355–1366, https://doi.org/10.5194/acp-11-1355-2011, https://www.atmos-chem-phys.net/11/1355/2011/, 2011.

Kiliani, J., Baumgarten, G., Lübken, F.-J., Berger, U., and Hoffmann, P.: Temporal and spatial characteristics of the formation of strong noctilucent clouds, J. Atmos. Solar-Terr. Phys., 104, 151–166, https://doi.org/10.1016/j.jastp.2013.01.005, 2013.

Klekociuk, A. R., Morris, R. J., and Innis, J. L.: First Southern Hemisphere common-volume measurements of PMC and PMSE, Geophys. Res. Lett., 35, L24804, https://doi.org/10.1029/2008GL035988, 2008.

Kopp, M., Gerding, M., Höffner, J., and Lübken, F.-J.: Tidal signatures in temperatures derived from daylight lidar soundings above Kühlungsborn (54°N, 12°E), J. Atmos. Solar-Terr. Phys., 127, 37–50, https://doi.org/10.1016/j.jastp.2014.09.002, 2015.

Kubo, K., Sugiyama, T., Nakamura, T., and Fukao, S.: Seasonal and interannual variability of mesospheric echoes observed with the middle and upper atmosphere radar during 1986 – 1995, Geophys. Res. Lett., 24, 1211–1214, https://doi.org/10.1029/97GL01063, 1997.

Latteck, R. and Bremer, J.: Long-term variations of polar mesospheric summer echoes observed at Andoya (69°N), J. Atmos. Solar-Terr. Phys., 163, 31 – 37, https://doi.org/https://doi.org/10.1016/j.jastp.2017.07.005, 2017.

Latteck, R., Singer, W., and Höffner, J.: Mesosphere summer echoes as observed by VHF radar at Kühlungsborn (54°N), Geophys. Res. Lett., 26, 1533–1536, https://doi.org/10.1029/1999GL900225, 1999.

Leslie, R. C.: Sky glows, Nature, 32, 245, 1885.

Li, Q., Rapp, M., Röttger, J., Latteck, R., Zecha, M., Strelnikova, I., Baumgarten, G., Hervig, M., Hall, C., and Tsutsumi, M.: Microphysical parameters of mesospheric ice clouds derived from calibrated observations of polar mesosphere summer echoes at Bragg wavelengths of 2.8 m and 30 cm, J. Geophys. Res., 115, D00I13, https://doi.org/10.1029/2009JD012271, 2010.

Lübken, F.-J., Baumgarten, G., Fiedler, J., Gerding, M., Höffner, J., and Berger, U.: Seasonal and latitudinal variation of noctilucent cloud altitudes, Geophys. Res. Lett., 35, L06801, https://doi.org/10.1029/2007GL032281, 2008.

Morris, R. J., Murphy, D. J., Klekociuk, A. R., and Holdsworth, D. A.: First complete season of PMSE observations above Davis, Antarctica, and their relation to winds and temperatures, Geophys. Res. Lett., 34, L05805, https://doi.org/10.1029/2006GL028641, 2007.

Muraoka, Y., Sugiyama, T., Sato, T., Tsuda, T., and Fukao, S.: Interpretation of layered structure in mesospheric VHF echoes induced by an inertia gravity wave, Radio Science, 24, 393–406, https://doi.org/10.1029/RS024i003p00393, 1989.

Nielsen, K., Nedoluha, G. E., Chandran, A., Chang, L. C., Barker-Tvedtnes, J., Taylor, M. J., Mitchell, N. J., Lambert, A., Schwartz, M. J., and III, J. M. R.: On the origin of mid-latitude mesospheric clouds: The July 2009 cloud outbreak, J. Atmos. Solar-Terr. Phys., 73, 2118 – 2124, https://doi.org/https://doi.org/10.1016/j.jastp.2010.10.015, 2011.

Nussbaumer, V., Fricke, K. H., Langer, M., Singer, W., and von Zahn, U.: First simultaneous and common volume observations of noctilucent clouds and polar mesosphere summer echoes by lidar and radar, J. Geophys. Res., 101, 19 161–19 167, 1996.

Ogawa, T., Kawamura, S., and Murayama, Y.: Mesosphere summer echoes observed with VHF and MF radars at Wakkanai, Japan (45.4°N), J. Atmos. Solar-Terr. Phys., 73, 2132 – 2141, https://doi.org/https://doi.org/10.1016/j.jastp.2010.12.016, 2011.

Rapp, M. and Lübken, F.-J.: Polar mesosphere summer echoes (PMSE): Review of observations and current understanding, Atmos. Chem. Phys., 4, 2601–2633, 2004.

Rapp, M. and Thomas, G. E.: Modeling the microphysics of mesospheric ice particles: Assessment of current capabilities and basic sensitivities, J. Atmos. Solar-Terr. Phys., 68, 715–744, https://doi.org/10.1016/j.jastp.2005.10.015, 2006.

Russell, J. M., Rong, P., Hervig, M. E., Siskind, D. E., Stevens, M. H., Bailey, S. M., and Gumbel, J.: Analysis of northern midlatitude noctilucent cloud occurrences using satellite data and modeling, J. Geophys. Res., 119, 3238–3250, https://doi.org/10.1002/2013JD021017, 2014.

Stevens, M. H., Lieberman, R. S., Siskind, D. E., McCormack, J. P., Hervig, M. E., and Englert, C. R.: Periodicities of polar mesospheric clouds inferred from a meteorological analysis and forecast system, J. Geophys. Res., 122, 4508–4527, https://doi.org/10.1002/2016JD025349, 2017.

Stober, G., Jacobi, C., Matthias, V., Hoffmann, P., and Gerding, M.: Neutral air density variations during strong planetary wave activity in the mesopause region derived from meteor radar observations, J. Atmos. Solar-Terr. Phys., 74, 55–63, https://doi.org/10.1016/j.jastp.2011.10.007, 2012.

Stober, G., Matthias, V., Jacobi, C., Wilhelm, S., Höffner, J., and Chau, J. L.: Exceptionally strong summer-like zonal wind reversal in the upper mesosphere during winter 2015/16, Ann. Geophys., 35, 711–720, https://doi.org/10.5194/angeo-35-711-2017, 2017.

Thomas, G. E.: Are noctilucent clouds harbingers of global change in the middle atmosphere ?, Adv. Space Res., 32, 1737–1746, https://doi.org/10.1016/S0273-1177(03)90470-4, 2003.

Thomas, L., Marsh, A. K. P., Wareing, D. P., and Hassan, M. A.: Lidar observations of ice crystals associated with noctilucent clouds at middle latitudes, Geophys. Res. Lett., 21, 385–388, 1994.

Thomas, L., Marsh, A. K. P., Wareing, D. P., Astin, I., and Chandra, H.: VHF echoes from the midlatitude mesosphere and the thermal structure observed by lidar, Journal of Geophysical Research: Atmospheres, 101, 12 867–12 877, https://doi.org/10.1029/96JD00218, 1996.

von Zahn, U. and Bremer, J.: Simultaneous and common-volume observations of noctilucent clouds and polar mesosphere summer echoes, Geophys. Res. Lett., 26, 1521–1524, https://doi.org/10.1029/1999GL900206, 1999.

von Zahn, U. and Höffner, J.: Mesopause temperature profiling by potassium lidar, Geophys. Res. Lett., 23, 141–144, https://doi.org/10.1029/95GL03688, 1996.

Wickwar, V. B., Taylor, M. J., Herron, J. P., and Martineau, B. A.: Visual and lidar observations of noctilucent clouds above Logan, Utah, at 41.7°N, J. Geophys. Res., 107, ACL 2/1–7, https://doi.org/10.1029/2001JD001180, 2002.

Zecha, M., Bremer, J., Latteck, R., Singer, W., and Hoffmann, P.: Properties of midlatitude mesosphere summer echoes after three seasons of VHF radar observations at 54°N, J. Geophys. Res., 108, 8439, https://doi.org/10.1029/2002JD002442, 2003.

Zeller, O., Hoffmann, P., Bremer, J., and Singer, W.: Mesosphere summer echoes, temperature, and meridional wind variations at mid- and polar latitudes, J. Atmos. Solar-Terr. Phys., 71, 931 – 942, https://doi.org/10.1016/j.jastp.2009.03.013, 2009.